AGU PUBLICATIONS

Earth's Future

RESEARCH ARTICLE
10.1002/2017EF000628

The Biosphere Under Potential Paris Outcomes

Sebastian Ostberg[1,2], Lena R. Boysen[1,3], Sibyll Schaphoff[1], Wolfgang Lucht[1,2], and Dieter Gerten[1,2]

[1]Earth System Analysis, Potsdam Institute for Climate Impact Research (PIK), Member of the Leibniz Association, Potsdam, Germany, [2]Geography Department, Humboldt-Universität zu Berlin, Berlin, Germany, [3]Land in the Earth System, Max Planck Institute for Meteorology, Hamburg, Germany

Key Points:
- A comprehensive analysis of land use and climate change as pressures on the biosphere is performed
- Historically, land use change has been the main driver of anthropogenic ecosystem change
- Climate change will likely take over as the main driver of ecosystem change during the 21st century

Supporting Information:
- Supporting Information S1.

Correspondence to:
Sebastian Ostberg,
ostberg@pik-potsdam.de

Citation:
Ostberg, S., Boysen, L. R., Schaphoff, S., Lucht, W., & Gerten, D. (2018). The Biosphere Under Potential Paris Outcomes, *Earth's Future*, *6*, 23–39, https://doi.org/10.1002/2017EF000628

Received 16 JUN 2017
Accepted 17 NOV 2017
Accepted article online 4 DEC 2017
Published online 9 JAN 2018

Abstract Rapid economic and population growth over the last centuries have started to push the Earth out of its Holocene state into the Anthropocene. In this new era, ecosystems across the globe face mounting dual pressure from human land use change (LUC) and climate change (CC). With the Paris Agreement, the international community has committed to holding global warming below 2°C above preindustrial levels, yet current pledges by countries to reduce greenhouse gas emissions appear insufficient to achieve that goal. At the same time, the sustainable development goals strive to reduce inequalities between countries and provide sufficient food, feed, and clean energy to a growing world population likely to reach more than 9 billion by 2050. Here, we present a macro-scale analysis of the projected impacts of both CC and LUC on the terrestrial biosphere over the 21st century using the Representative Concentration Pathways (RCPs) to illustrate possible trajectories following the Paris Agreement. We find that CC may cause major impacts in landscapes covering between 16% and 65% of the global ice-free land surface by the end of the century, depending on the success or failure of achieving the Paris goal. Accounting for LUC impacts in addition, this number increases to 38%–80%. Thus, CC will likely replace LUC as the major driver of ecosystem change unless global warming can be limited to well below 2°C. We also find a substantial risk that impacts of agricultural expansion may offset some of the benefits of ambitious climate protection for ecosystems.

Plain Language Summary Ecosystems across the world are under increasing pressure from man-made climate change and humanity's use of land for agriculture. While countries have agreed to limit climate change to less than 2 degrees in the 2015 Paris Agreement the success of climate protection is currently uncertain. At the same time, continued population growth is causing demand for food and bioenergy to rise. We use computer simulations to explore which ecosystems are at risk of major change due to climate change and land use by the end of the 21st century. We find that climate change could transform between 16% and 65% of all ecosystems worldwide substantially, depending on how successful greenhouse gas emissions can be reduced. 11% to 25% of ecosystems may also experience severe impacts from land use, depending on how much land is needed for agriculture. In the worst case we studied, climate change and land use change risk transforming up to 80% of the land biosphere into a completely new state, putting many species at risk of extinction if they cannot adapt to their rapidly changing environment.

1. Introduction

With the Industrial Revolution, humans have emerged as a major driver of change in the Earth system, prompting the advent of the Anthropocene (Steffen et al., 2007). Today, 7.5 billion people rely on the biosphere to supply them with a multitude of essential ecosystem services (Millennium Ecosystem Assessment, 2005; UNPD, 2015). For the purpose of food production alone, roughly 1500 Mha of land are used to grow crops, and twice as much grazing land feeds cattle, sheep, and other livestock (FAO, 2016). Three quarters of the land surface show signs of human alteration as they are either used directly or have become embedded within agricultural land or settlements (Ellis et al., 2010). Land use in combination with humanity's utilization of fossil fuels has released a total of 565 ± 55 Gt carbon into the atmosphere between 1870 and 2016 and has increased atmospheric CO_2 concentration from ≈278 ppm at the beginning of the industrial era (1750) to 403 ppm in 2016 (Dlugokencky & Tans, 2017; Joos & Spahni, 2008; Le Quéré et al., 2016). The resultant

global warming has crossed 1 K above the 1880–1900 global annual average surface temperature in 2015 (GISTEMP Team, 2017; Hansen et al., 2010), reaching the half point to the 2°C limit set by the international community in the Paris Agreement (UNFCCC, 2016). Taking the Paris Agreement into account, three outcomes for the 21st century can be imagined: (1) assuming a full success, global warming will be limited to well below 2°C above preindustrial, (2) emissions will be reduced, but not enough to limit global warming to 2°C, (3) in case of a widespread failure of the Paris Agreement emissions continue to rise unabated.

Given that global population and its food demand is still on the rise, and taking into account the inertia of the climate system, pressure on the biosphere from land use change (LUC) and climate change (CC) is likely to increase over the course of the 21st century even in the best of these three cases. Furthermore, as pointed out by Rockström et al. (2016), negative greenhouse gas (GHG) emissions are a key requirement of most recent scenarios assessed by the Intergovernmental Panel on Climate Change (IPCC) that attempt to limit warming to below 2°C (IPCC, 2014). Usually, these scenarios rely on bioenergy with carbon capture and storage (BECCS) to deliver a carbon sink in the order of magnitude of the global ocean sink (Rockström et al., 2016). As such, reducing one pressure on the biosphere (CC) may directly exacerbate the other (LUC).

Although impacts of CC and LUC on ecosystems have been documented for every continent and major biome, quantifying them in a comprehensive, consistent and comparable manner across the globe for both past and future changes still poses methodological challenges. Ellis and Ramankutty (2008) proposed to map the historical anthropogenic transformation of the biosphere by way of anthropogenic biomes or "anthromes", recognizing that human impacts extend beyond the land used directly to create a number of seminatural systems. Changes in 21st century land cover driven by CC and LUC have been studied before for a subset of the Representative Concentration Pathways (RCPs) (Boit et al., 2016; Davies-Barnard et al., 2015). For our study, a more complex model-based indicator of human interference with the biosphere at the landscape level (Heyder et al., 2011; Ostberg et al., 2015) is used to estimate how much CC and LUC impact landscapes worldwide individually and in their interaction during the historical period (20th century) and for a set of CC and associated LUC scenarios representative of the three outlined Paris outcomes (21st century). The analysis compares the relative strength of CC and LUC effects and their joint impact on the terrestrial biosphere and highlights the consequences of different levels of CC mitigation. We further investigate whether trade-offs between CC and LUC impacts emerge in the scenarios based on different strategies of future land use. This study expands on the comparison of historical CC and LUC impacts on the biosphere presented in Ostberg et al. (2015).

Emissions reductions pledged by countries in order to achieve the 2°C target, so-called Intended Nationally Determined Contributions (INDCs), only cover the period up to 2030, so any assessment of long-term climate impacts is highly dependent on assumptions about how emissions develop thereafter. Preliminary analysis of the INDCs suggests that they will likely not be sufficient to limit warming to below 2°C unless mitigation efforts are stepped up considerably after 2030 (e.g., Fawcett et al., 2015; Rogelj et al., 2016; UNFCCC, 2015). While simple reduced-complexity climate models have been used to estimate global average temperature rise resulting from a range of INDC extensions (e.g., Climate Action Tracker, http://www.climateactiontracker.org/), these do not provide spatial patterns of temperature change or changes in other climate variables which are required for an impact assessment. For this study, we use climate projections produced by a large number of climate and Earth system models as part of the fifth phase of the Coupled Model Intercomparison Project (CMIP5, Taylor et al., 2012) and based on the RCPs (van Vuuren et al., 2011a). Although developed independently of the Paris process, RCP2.6 is used here to represent a "Paris success." RCP4.5 is used as a proxy for an "INDC+" world where mitigation efforts are increased somewhat over INDC levels, but not enough to safely stay within the 2° limit. RCP6.0 is used to represent an "INDC" world where efforts after 2030 continue the 2020–2030 trends. These three scenarios lead to 1.6 ± 0.4 K (multimodel mean and standard deviation), 2.4 ± 0.5 K and 2.8 ± 0.5 K of global warming in 2081–2100 compared to the average global mean temperature in 1850–1900, respectively (Collins et al., 2013). Lastly, RCP8.5 is used as a proxy for a "Paris failure" scenario. Assuming continued high GHG emissions in the absence of effective mitigation, this pathway leads to 4.3 ± 0.7 K of global warming by the end of the century.

The RCPs are based on a set of Integrated Assessment Model (IAM) scenarios which also include scenarios of future land use consistent with the climate projections (Hurtt et al., 2011). For this study, each RCP CC

scenario is combined with the respective LUC scenario (see Subsection 2.3 below for a characterization of LUC forcing in each scenario).

For the quantification of terrestrial biospheric change, each landscape is treated as a point in a multidimensional state space that gets shifted from its reference conditions to a new state by CC and LUC (Heyder et al., 2011; Ostberg et al., 2015). In this context, a landscape is defined as a contiguous area of land which may feature both natural vegetation and managed land — similar to the anthrome concept — but is characterized by homogeneous weather conditions and represented by a grid cell in the model (see "Methods" below). The distance between two positions in the state space describes the level of human interference with the biosphere in each landscape. The Γ metric used here combines changes in biogeochemical processes and vegetation structure to quantify changes in landscape states (see Table S1 in the Supporting Information S1 for the full list of parameters). These parameters serve as a proxy for several ecosystem services, such as food production (harvest), carbon sequestration (carbon stocks), and freshwater provisioning (runoff). Although they represent rather broad biogeochemical and structural properties, changes to these fundamental building blocks imply a risk of substantial, potentially self-amplifying transformations in the underlying, much more complex system characteristics, food chains and species composition, with possible implications for biodiversity (Heyder et al., 2011).

The Γ metric is a unit-less number scaled between 0 (no change) and 1 (very strong change, see Methods below). Following previous applications (e.g., Heyder et al., 2011; Ostberg et al., 2013, 2015), $\Gamma < 0.1$ is considered a minor, values between 0.1 and 0.3 a moderate and $\Gamma > 0.3$ a major landscape change. For illustrative purposes, the difference between present-day biomes generally adopts values of $\Gamma > 0.3$, such as a tropical rainforest changing into a tropical seasonal forest (~0.30), a tropical savanna (~0.5–0.7) or a grassland (~0.85); or a boreal forest changing into a temperate forest (~0.3–0.4) or a temperate savanna (~0.5–0.6), whereas moderate changes may be compared in magnitude to the difference between similar biomes, such as a temperate coniferous forest and a temperate broadleaved forest (~0.1–0.2) (Ostberg et al., 2013). For LUC impacts, the magnitude of change depends on a number of factors such as the fraction of the grid cell that is transformed, the vegetation type that is replaced, and land use type and history, with major impacts ($\Gamma > 0.3$) calculated for landscapes where more than 40%–60% of the area have been converted to land use (Ostberg et al., 2015).

2. Methods

The Γ metric of the risk of landscape-level biogeochemical change is used here to assess systematically the dual pressure from LUC and CC on the biosphere. It captures five dimensions of change (Heyder et al., 2011; Ostberg et al., 2015):

$$\Gamma = \left(\Delta V \cdot S\left(\Delta V, \sigma_{\Delta V}\right) + c \cdot S\left(c, \sigma_c\right) + g \cdot S\left(g, \sigma_g\right) + b \cdot S\left(b, \sigma_b\right)\right)/4 \quad (1)$$

ΔV quantifies the structural dissimilarity between two landscape states in terms of basic plant life forms (trees, grass, or bare ground) and their attributes (modified after Sykes et al., 1999, see Text S1 in the Supporting Information S1). *S*, *c*, *g*, and *b* are calculated in the multidimensional state space characterized by the biogeochemical properties in Table S1 in the Supporting Information S1.

Local change *c* quantifies relative changes in biogeochemical stocks and fluxes compared to local reference conditions in each landscape, represented by a grid cell in the model (see below).

By comparing local changes to the global mean reference conditions, global importance *g* captures the varying contribution of each grid cell to global biogeochemical cycles, taking into account that even moderate (relative) changes on the local scale may feed back to larger scales if large enough in absolute terms.

Ecosystem balance *b*, which is calculated as the angle between state vectors, quantifies shifts in the relative magnitude of biogeochemical properties with respect to each other as an indicator for qualitative changes in the balance of dynamic processes, which may signal a breakdown of ecological functioning.

S evaluates the change in each of the previous four components in comparison to its interannual variability σ under reference conditions, based on the assumption that ecosystems are adapted to the variability they are regularly exposed to but may be vulnerable if it is exceeded.

For more details about the vector geometry and the sigmoid transformation functions used to scale *S*, *c*, and *g* between 0 and 1, see Text S2 in the Supporting Information S1 and Heyder et al. (2011).

The LPJmL dynamic global vegetation model is used to simulate landscape states and their evolution through CC and LUC, providing all parameters in Table S1 in the Supporting Information S1. LPJmL is well-established and has been extensively documented before so the following is only a short summary. The model simulates key ecosystem processes such as photosynthesis, plant and soil respiration, carbon allocation, evapotranspiration and phenology for natural vegetation represented by nine plant-functional types (PFTs) (Sitch et al., 2003), agricultural production represented by 12 crop-functional types (CFTs) and managed grassland (Bondeau et al., 2007), as well as dedicated biomass plantations (for bioenergy) using two woody and one herbaceous biomass-functional types (BFTs) (Beringer et al., 2011). In each grid cell PFTs compete for light, space, and water. Their establishment is constrained by climatic suitability and the density of the existing vegetation, whereas their mortality depends on climatic stress (i.e., heat), plant density and growth efficiency (Sitch et al., 2003). Fire disturbance in natural vegetation is simulated using the Glob-FIRM fire model (Thonicke et al., 2001), which estimates day-to-day fire probability based on litter moisture and the annual burned fraction of the grid cell based on the length of the fire season. The LPJmL model version used here includes a five-layer soil hydrology and permafrost module (Schaphoff et al., 2013). CFTs, managed grassland and BFTs are grown on prescribed areas (see section on land use data below), with a distinction between rain-fed and irrigated agriculture. Irrigation is possible on prescribed areas equipped for irrigation, with water demand derived from the soil water deficit below optimal growth (Rost et al., 2008). To provide a better representation of irrigation efficiency, i.e., the partitioning of water withdrawn into beneficial consumption by the plant and conveyance and application losses, the model distinguishes three major irrigation systems (surface, sprinkler, and drip) (Jägermeyr et al., 2015). Sowing dates for annual crops are computed internally based on a set of rules depending on crop- and climate-specific characteristics (Waha et al., 2012), and crops are harvested after reaching a crop-specific phenological heat unit sum. Crop residues are left on the field, and extensive grass growth is simulated outside the growing period of annual crops as a proxy for inter-cropping practices (Bondeau et al., 2007). Other aspects of crop management, fertilizer application or soil fertility management are not explicitly modeled. To account for nonclimatic factors influencing agricultural intensities maximum leaf area index (LAI_{max}) of each CFT is calibrated to best match FAOSTAT national yields at the country level (Fader et al., 2010). Managed grassland is harvested monthly, with global harvest tuned to fulfill present-day global feed demand for livestock production and harvest fraction in each grid cell dependent on local productivity. Depending on the scenario, bioenergy plantations are either stocked with highly productive C4 grasses or broadleaved trees (representative of willow/poplar for the temperate zone and eucalyptus for the tropics). 85% of the leaf mass of bioenergy grasses is harvested once or several times a year when leaf carbon stocks reach 400 g/m^2, whereas bioenergy trees are managed as short-rotation coppice systems harvested every eight years (Heck et al., 2016). The model runs at a daily time step and a spatial resolution of 0.5° by 0.5°. It is driven by monthly fields of cloud cover, precipitation, and temperature which are disaggregated to daily values following Gerten et al. (2004).

2.1. Input Data

Climate input is created from all climate models from the CMIP5 archive that provide all required variables for the historical period and all four RCP scenarios (20 models in total, https://pcmdi.llnl.gov/projects/cmip5/). In a first step, raw climate model output is interpolated to a 0.5° by 0.5° resolution by bilinear interpolation. Next, simulated time series of each variable are corrected for systematic errors in mean and variance applying a quantile mapping approach based on the method described in Watanabe et al. (2012). While the original approach was developed for the bias correction of time slices, the required statistics (mean and variance) are calculated for each time step applying a moving 31-year window. Obtained statistics are compared to climate observations for the reference period 1970–2000 to derive correction offsets (temperature) and correction factors (cloud cover, precipitation, all variances). Observational reference data are taken from the Climatic Research Unit's time-series (CRU TS) 3.21 datasets (Harris et al., 2014; University of East Anglia Climatic Research Unit et al., 2013) for temperature and cloud clover and from the Global Precipitation Climatology Centre's (GPCC) full data reanalysis version 6 (Becker et al., 2013; Schneider et al., 2011) for precipitation. Wet-day frequency, which is used by LPJmL to distribute monthly precipitation sums, is created synthetically following Heinke et al. (2013) since it is not provided directly by the climate models.

Annual midyear atmospheric CO_2 concentrations for both the historical period and all four RCP scenarios are taken from the RCP database (http://tntcat.iiasa.ac.at/RcpDb).

Land use input is based on the land use harmonization (LUH) products created for CMIP5 (Hurtt et al., 2011, available at http://luh.umd.edu/data.shtml). The LUH dataset provides gridded annual fractions of total cropland (LUH variable g_{crop}) and managed grassland (g_{past}) at a spatial resolution of 0.5° by 0.5°, which have been harmonized to provide a smooth transition from the historical period (1700–2004) to each of the four RCP scenarios (2005–2100). In addition, LUH provides gridded information on biofuels (g_{biof}) in each scenario. LPJmL distinguishes 12 CFTs and an "others" category containing the remaining cropland, and also separates rain-fed from irrigated cropland. To add this information to the LUH dataset, it is combined with the default LPJmL historical dataset (Fader et al., 2010), which is derived from a combination of crop-specific rain-fed and irrigated harvested areas (MIRCA2000, Portmann et al., 2010), historical trends in cropland and managed grassland (HYDE3, Klein Goldewijk & van Drecht, 2006) and historical trends in irrigated areas (Hoekstra, 1998). In case of inconsistencies between both historical datasets, managed grassland fractions are taken directly from g_{past}. For cropland, relative CFT shares in each grid cell of the LPJmL default dataset CFT_{LPJmL} are rescaled proportionally to match total cropland from LUH g_{crop}:

$$CFT_{LUH} = \frac{CFT_{LPJmL}}{cropland_{LPJmL}} \cdot g_{crop} \quad (2)$$

To preserve irrigated areas, changes are preferentially applied to the rain-fed cropland share. Grid cells missing in the LPJmL default dataset but containing cropland in LUH are filled using the country-average CFT mix from the LPJmL default dataset. For the four RCP scenarios, the present-day CFT mix in each grid cell remains constant and is rescaled proportionally to match future total cropland g_{crop} following Equation 2. Irrigated cropland is scaled proportionally with total cropland since the RCP scenarios do not include information on irrigated land. Future managed grassland fractions g_{past} are taken directly from LUH.

Subregional information on the global distribution of irrigation systems is available neither for the historical period nor the future scenarios. Following the approach in Jägermeyr et al. (2015), country-level shares of irrigation systems from AQUASTAT (FAO, 2014) are disaggregated to grid cells and CFTs through a decision tree approach, using the extent of irrigated areas by CFT and an irrigation system suitability table (full description in Jägermeyr et al., 2015).

The LUH biofuel information g_{biof} was not part of the original harmonization process, but was added to the LUH dataset at a later stage. For RCP2.6, RCP4.5, and RCP6.0 g_{biof} represents a land fraction that has to be subtracted from total cropland g_{crop}. CFT fractions are scaled down proportionally to make room for bioenergy. In cases where g_{biof} is larger than g_{crop} (because of the missing harmonization), preference is given to g_{biof}, which is then expanded into g_{past} and (if not sufficient) into natural vegetation. For RCP2.6 and RCP6.0 g_{biof} in each grid cell is split equally between bioenergy grass and bioenergy tree (short-rotation coppice) plantations, except for cells where climate conditions prohibit tree growth (see Text S3 in the Supporting Information S1 for details). For RCP4.5 the LUH documentation specifies bioenergy crops to be herbaceous so g_{biof} is assigned completely to the bioenergy grass BFT in LPJmL. For RCP8.5 g_{biof} represents gridded harvested biomass amounts instead of land fractions. Bioenergy fractions in each grid cell g^*_{biof} are derived under the assumption that they are proportional to the bioenergy harvest share of total wood harvest:

$$g^*_{biof} = \frac{g_{biof}}{harvest_{wood}} \cdot frac_{wood} \quad (3)$$

with $harvest_{wood}$ the sum of LUH variables g_{sbh1}, g_{sbh2}, g_{sbh3}, g_{vbh1}, and g_{vbh2} (wood harvested from different sources) and $frac_{wood}$ the sum of LUH variables g_{fsh1}, g_{fsh2}, g_{fsh3}, g_{fvh1}, and g_{fvh2} (land fractions corresponding to harvested biomass). Short-rotation coppice plantations are simulated on all RCP8.5 bioenergy land fractions, which reduce the area available for natural vegetation. No irrigation is applied to bioenergy plantations in any of the RCP scenarios to avoid competition with food production for available irrigation water. Grid cell fractions not covered by cropland, managed grassland, bioenergy plantations or water are simulated with natural vegetation.

Additional inputs to LPJmL include a flow direction map (STN-30, Vörösmarty et al., 2000) and a database of the location and storage capacity of dams and reservoirs (GRanD, Lehner et al., 2011), both of which affect

the routing of discharge through the river network (Biemans et al., 2011; Rost et al., 2008), a gridded dataset of lake and river fractions based on the Global Lakes and Wetlands Database (Lehner & Döll, 2004) which affects the land area available in each grid cell. Soil data describing the thermal and hydraulic characteristics are taken from the Harmonized World Soil Database (version 1.2) (FAO et al., 2012) and classified according to the USDA soil texture classification (http://ufdc.ufl.edu/IR00003107/00001).

2.2. Simulation Setup

To allow for the individual evaluation of CC and LUC effects as well as their combined impact on the biosphere, four parallel lines of simulations are conducted for each climate model (bottom-left schematic in Figure 1): PNV_{CC} and PNV_{noCC} simulations feature no land use, with all the ice-free land surface covered with potential natural vegetation (PNV). LUC_{CC} and LUC_{noCC} simulations include land use using historical and future scenario land use patterns described above. PNV_{noCC} and LUC_{noCC} simulations use a constant historical climate and a constant preindustrial CO_2 concentration of 278 ppm until 2099. They provide the reference conditions for the full impact and CC effect, respectively. PNV_{CC} and LUC_{CC} simulations use transient climate and transient atmospheric CO_2 concentrations. PNV_{CC} provides reference conditions for the land use change effect, whereas LUC_{CC} represents the real world which is compared to each of the three reference simulations. Land use scenarios start to diverge in 2005, but because of the 31-year moving window used in bias correction climate scenarios may start to diverge slightly from as early as 1991. All scenarios are run until 2099.

All simulations are preceded by 5000 years of spin up to allow vegetation and soil carbon pools to reach an equilibrium state. Spin up is performed for each GCM separately with dynamic vegetation and fire disturbance enabled, but without any land use. The first 30 years of 20th century climate are randomly sampled into a 200-year sequence, which is recycled repeatedly during spin up, together with a constant preindustrial CO_2 concentration of 278 ppm. From there, LUC_{CC} and LUC_{noCC} simulations add another 100 years of land use spin up using year-1700 land use patterns to adjust carbon pools before using transient historical land use patterns from 1700 onward.

LAI_{max} calibration of yields is performed on a decadal basis for five decades from 1961 to 2010 for which FAOSTAT national yield statistics are available (FAO, 2016), using the observational climate data sets from bias correction to drive the model. Historical trends in agricultural intensity are derived by linear regression for each country and each CFT and are then extrapolated into the future with a maximum upper limit of $LAI_{max} = 7$. For countries with negative historical trends, these are reversed in the future. This procedure introduces some agricultural intensification in the future, but is not intended to reproduce productivity increases assumed in each of the original IAM scenarios the RCPs are based on. While management intensity has an impact on the Γ metric Ostberg et al. (2015) showed that its effect is minor compared to the first-order effect of changing natural vegetation into cropland/managed grassland.

Time series of Γ for each climate model are derived by comparing 30-year moving windows of LUC_{CC} simulations to concurrent windows in the three reference runs LUC_{noCC}, PNV_{CC} and PNV_{noCC}. ΔV, c, g, and b from Equation 1 are calculated from the window mean while S is estimated from the interannual variability within the 30-year window.

2.3. CC and LUC Forcing in the RCPs

Radiative forcing in the RCP2.6 scenario used here to represent a *Paris success* peaks before mid-century and then declines to 2.6 W/m^2 by 2100. CO_2 emissions in the less ambitious *INDC+* and *INDC* scenarios peek roughly 20 (RCP4.5) and 40 years (RCP6.0) later than in the *Paris success* case, and radiative forcing stabilizes only after 2100 at 4.5 and 6 W/m^2, respectively (van Vuuren et al., 2011a). Out of the three scenarios, only RCP2.6 is likely to achieve the ultimate goal of the Paris Agreement of limiting global warming to below 2°C (Collins et al., 2013). CO_2 emissions in the illustrative *Paris failure* (RCP 8.5) scenario keep rising throughout the 21st century, and radiative forcing reaches 8.5 W/m^2 in 2100, with a stabilization only after 2200. All four scenarios analyzed in this study project an increase of global population combined with an increase in per capita food demand and feature an increasing contribution of biofuels to the global energy mix (van Vuuren et al., 2011a). Despite these similarities, their global land use area varies between roughly 3700 and more than 6000 Mha in 2100 (Table 1). Besides total area, the scenarios differ in terms of the relative share of cropland, managed grassland, and bioenergy plantations and regarding the placement of land use (Figure S1 in

Table 1.
Global land area (Mha) covered by major types of managed land in 2004 and in 2100 under four studied Paris outcomes. Bioenergy refers to dedicated second-generation biomass plantations

Year/scenario	Pasture	Cropland	Bioenergy	Total
2004	3334	1519	0	4853
Paris success (RCP 2.6)	3149	1869	441	5459
INDC+ (RCP 4.5)	2861	783	295	3939
INDC (RCP 6.0)	1766	1582	338	3686
Paris failure (RCP 8.5)	3702	1800	543	6045

the Supporting Information S1). Total managed land expands by 606 Mha compared to 2004 under the *Paris success* (RCP2.6) scenario, due to a 23% increase of global cropland and the introduction of almost 450 Mha of dedicated biomass plantations for bioenergy production (corresponding to ∼30% of current cropland). While the *INDC+* and *INDC* scenarios represent an assumption of half-way success in climate mitigation both RCPs exhibit extreme success in reducing the concurrent land use pressure, leading to a net abandonment of 913 and 1166 Mha of managed land, respectively. Strong increases in crop productivity and efficiency of food production assumed in the underlying IAM scenario allow for a reduction of global cropland by 48% under *INDC+* (RCP4.5) (Thomson et al., 2011), whereas *INDC* (RCP6.0) reduces grazing-based livestock production, leading to a net abandonment of 47% of global pastures (Masui et al., 2011). In addition to the highest CC forcing, the *Paris failure* (RCP8.5) scenario also features the largest expansion of managed land of all four scenarios (Table 1). The RCPs cover a wide range of assumptions regarding future yield gains, intensification of livestock production and dietary shifts (van Vuuren et al., 2011a). The land use patterns resulting from these assumptions are assessed here in terms of their impact on the biosphere.

3. Results

At the end of the historical period (1976–2005 time slice), human interference with the terrestrial biosphere through the interaction of CC and LUC has already caused major impacts ($\Gamma > 0.3$) in landscapes covering 25%–30% of the ice-free land surface (full impact in Figure 1, range across 20 climate models). Given that more than 75% of all landscapes worldwide contain some amount of managed land (Ellis et al., 2010, see also Figure S1 in the Supporting Information S1) the full impact is usually a combination of CC- and LUC-driven changes, but values of the individual effects are not necessarily additive: major CC and LUC effects can co-occur within the same landscape, but the full impact may also attain values of $\Gamma > 0.3$ in landscapes where both individual effects are below that threshold. Because of the complex way in which CC and LUC affect the individual parameters describing landscape states it is even possible for the full impact to be smaller than the individual effects. Globally, LUC is the main driver of change, responsible for major impacts on 18%–19% of the land surface compared to 5%–10% subject to major CC impacts (land use change effect and climate change effect in Figure 1, respectively).

3.1. Paris Success

In case of a *Paris success* (RCP2.6)—which would limit global warming to below 2°C above preindustrial level—major CC effects are limited mostly to cold (tundra, boreal forests) and dry regions (deserts and grasslands, Figure 2). They are still projected for 22% (16%–27% model range) of the global land surface by 2070–2099 (climate change effect, Figure 1), which represents a two to fivefold increase over the historical period. Even in this low warming scenario, tundra ecosystems may lose more than half of their preindustrial extent (Figure 3). Boreal forests are simulated to expand into the tundra, while on the other hand tree composition shifts toward temperate species along their warm edge (Figure S3 in the Supporting Information S1). Based on the RCP2.6 land use scenario, LUC is estimated to expose landscapes covering 23% of the land surface to major impacts by 2070–2099 (22%–25%, land use change effect, Figure 1), which roughly equals the extent of major CC impacts. Land use expansion is concentrated in tropical forests as well as tropical savannas and grasslands, where areas of major LUC effects expand by 59% (33%–74%) and 88% (51%–140%), respectively, compared to the historical period (Figure S5 in the Supporting Information S1). At the global scale, human interference with the biosphere through both CC and LUC is projected to

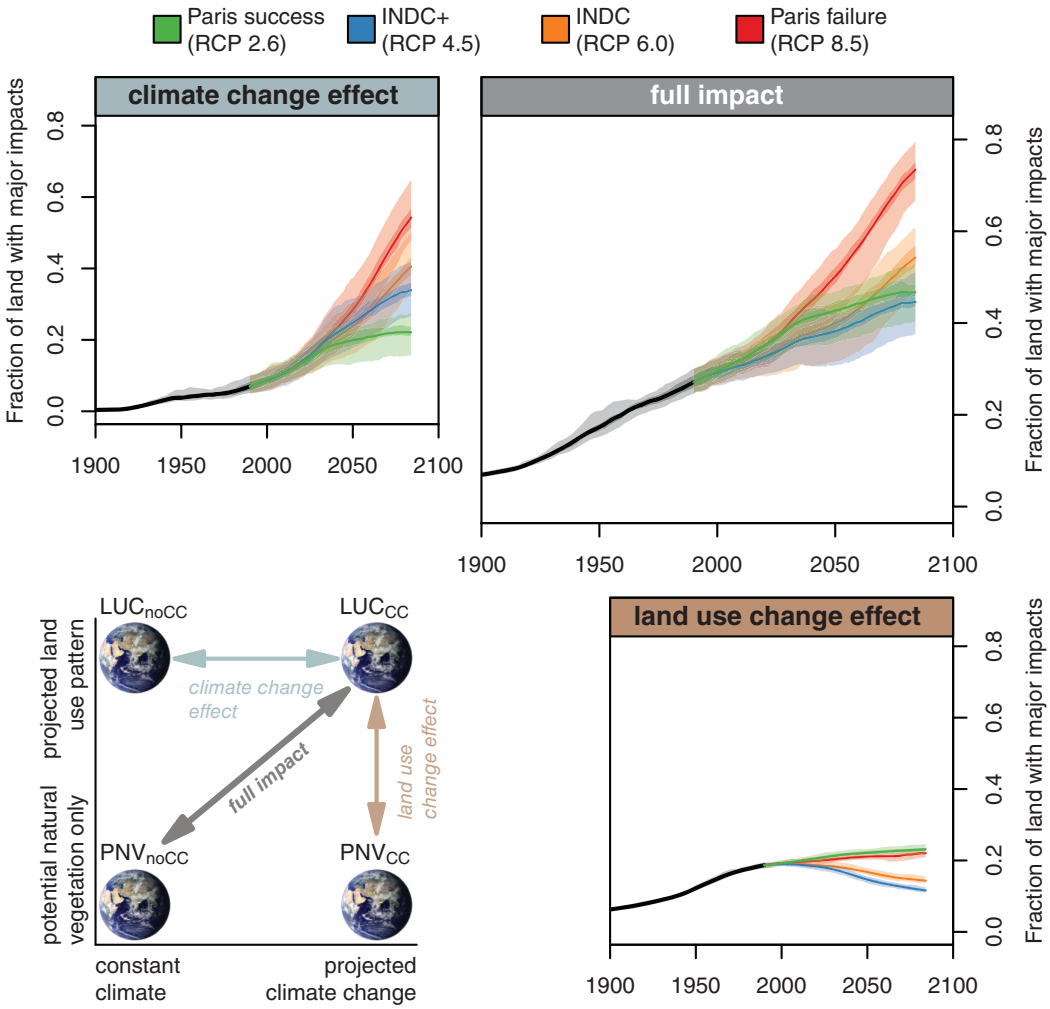

Figure 1. Fraction of the global land surface exposed to major landscape change under four studied Paris outcomes. The climate change effect and land use change effect measure the impact caused by climate change and land use change individually, while the full impact measures the combined effect, as illustrated by the schematic in the lower left and described in Subsection "Simulation setup". Colored lines show the ensemble mean of affected areas based on LPJmL simulations driven by 20 different climate models, while shaded areas show the inter-quartile range (dark shading) and full range (light shading) of simulations. Earth image by NASA Goddard Space Flight Center.

cause major changes on 47% of the land surface by 2070–2099 (40%–53%, full impact, Figure 1). At the biome level, the relative contributions of CC and LUC vary widely: For example, CC effects are generally low in tropical and temperate forests, but full impacts are in the same range as the global aggregate because of the high level of land use in these regions (Figure 3, Figures S5 and S6 in the Supporting Information S1). CC and LUC contribute roughly equally to major full impacts in tropical savannas and grasslands, but there is little spatial overlap between major impacts caused by both effects (Figure 2). In Asia and the western U.S., co-occurring minor or moderate CC and LUC effects amplify in temperate savannas and grasslands to cause major full impacts in roughly 46% more landscapes than the sum of both individual effects. A similar amplification effect is found in forests in Eastern Europe.

3.2. *INDC+* Scenario

Less ambitious CC mitigation under *INDC+* translates into considerably higher numbers of landscapes with major CC effects, eventually covering 34% (27%–42%) of the land surface by the end of the century (Figure 1). This represents a 54% (32%–83%) increase over the *Paris success* scenario and a four to sevenfold increase over the historical period (1976–2005). In cold biomes three quarters of climate models agree on major CC effects for more than 80% of the tundra and more than 40% of all boreal forests (Figure S6 in the

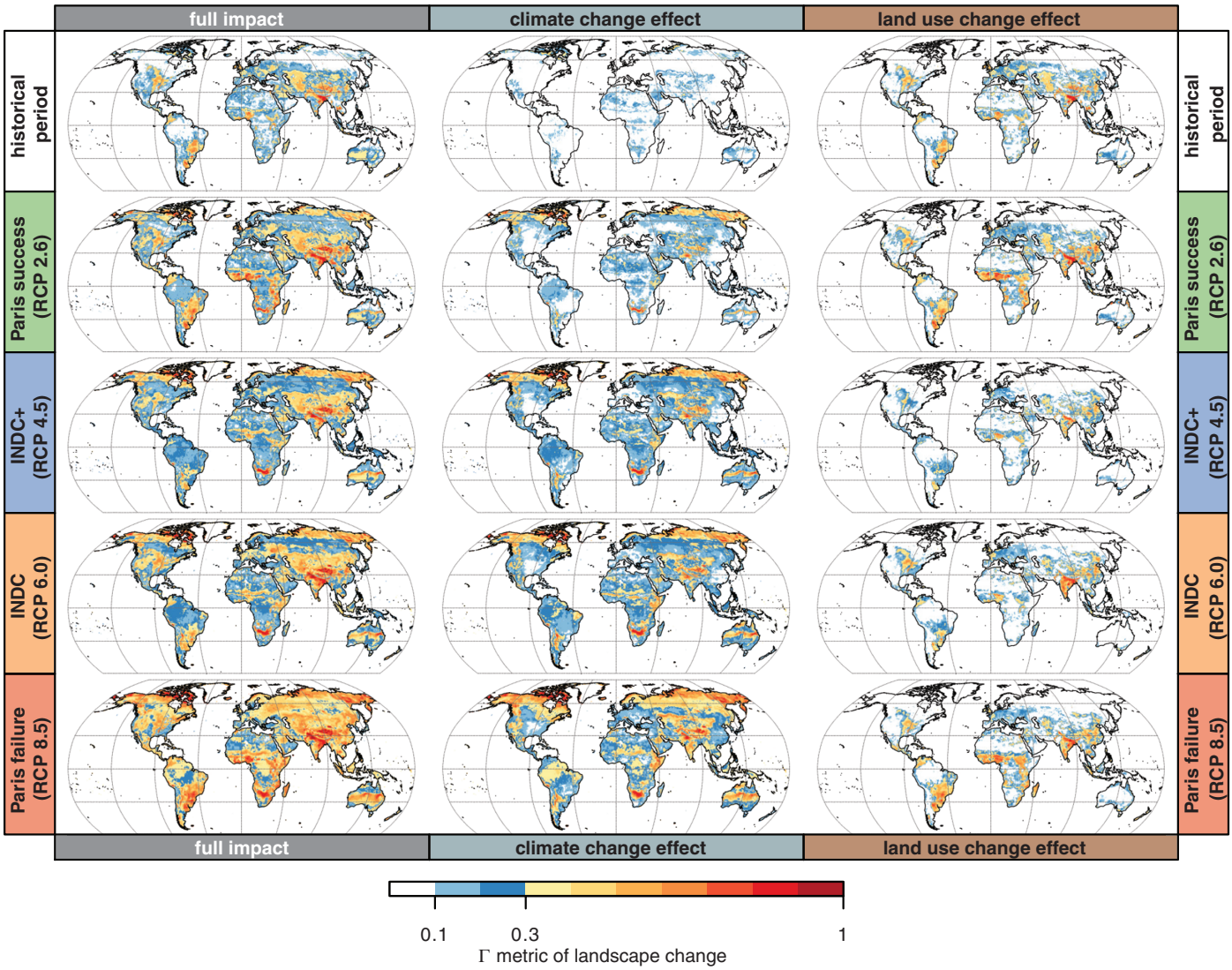

Figure 2. Simulated landscape change under four studied Paris outcomes. Maps show the ensemble mean across LPJmL simulations driven by 20 different climate models. Historical period refers to 1976–2005 while all scenarios refer to 2070–2099. Blue colors depict moderate ($0.1 < \Gamma < 0.3$) and yellow to red colors depict major landscape changes ($\Gamma > 0.3$).

Supporting Information S1). Changes in the high latitudes are not only driven by temperature rise, which extends the growing season length, but also by an increase in precipitation projected for that region. Major CC effects are also projected for roughly half of all tropical and one third of all temperate savannas and grasslands. For tropical forests, moderate CC effects ($0.1 < \Gamma < 0.3$) dominate, with major CC impacts projected for 14%–29%. CC impacts in temperate forest regions are still widely below the moderate threshold ($\Gamma < 0.1$, Figure 2). The underlying RCP4.5 scenario has a strong afforestation/avoided LUC emissions component to its emissions mitigation strategy (Thomson et al., 2011). After some land use expansion during the early 21st century, managed land is reduced in all biomes except tropical savannas (Figure S4 in the Supporting Information S1). At the global scale, landscapes with major LUC effects shrink from 18%–19% of the land surface in 1976–2005 to 11%–13% in 2070–2099. The fraction of the land surface exposed to major full impacts, i.e., the combination of CC and LUC, is almost identical in the *INDC+* and *Paris success* scenarios (45% and 47%, respectively, Figure 1) which can be traced back to the differences in land use: Compared to the *Paris success* scenario, *INDC+* reduces the extent of landscapes with major LUC effects by almost two thirds in tropical forests, and roughly 50% in most other biomes (Figure S5 in the Supporting Information S1). This higher pressure from LUC under the *Paris success* scenario is reflected in the joint full impact: *Paris success* exposes 52% (22%–81%) more tropical and 22% (11%–36%) more

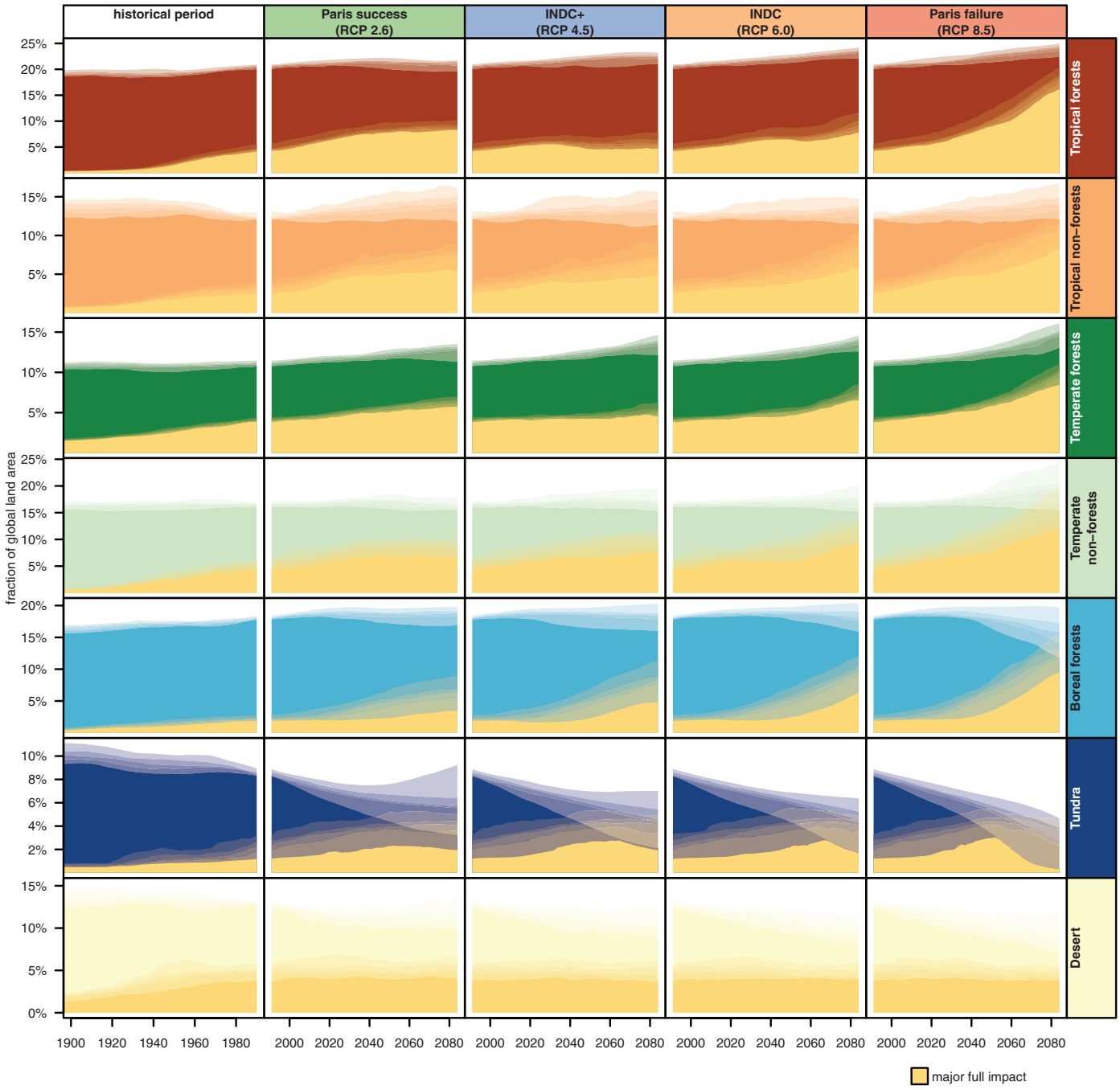

Figure 3. Joint full impacts of CC and LUC in major biomes over time. Each plot shows the fraction of the global land area covered by the respective biome as well as the fraction of the biome projected to experience major change (yellow overlay). Biome classification of landscapes (grid cells) is based on their potential natural vegetation even if land has been converted to agriculture. Semitransparent shading denotes climate model uncertainty (maximum extent, 75%, 50% and 25% quantile and minimum extent with increasing opacity). See Figures S5 and S6 in the Supporting Information S1 for corresponding versions showing the individual effects of LUC and CC.

temperate forest landscapes to major full impacts than *INDC*+ (Figure 3), even though major CC effects are simulated for two to five times and two to three times as many landscapes in tropical and temperate forests, respectively under *INDC*+ (Figure S6 in the Supporting Information S1).

3.3. *INDC* Scenario

Under *INDC* (RCP6.0), major CC effects are projected for 41% (34%–50%) of the land surface by 2070–2099, an 83% (62%–121%) increase over the *Paris success* scenario (Figure 1). The largest expansion of major

CC effects is projected for tropical forests, especially in Africa and South America (Figure 2). CC causes an expansion of tropical seasonal forests at the expense of both tropical evergreen forests and tropical savannas (Figure S3 in the Supporting Information S1). However, some of these areas, especially in Africa, are heavily used as pastures and cropland, which may suppress climate-driven forest expansion. In terms of LUC forcing, *INDC* has slightly less total managed land than *INDC+* (Table 1), but only the global pasture area is strongly reduced in this scenario, whereas croplands are relocated partially between biomes and overall expand by 4% globally. Cropland expansion takes place mostly in tropical and temperate forests (Figure S4 in the Supporting Information S1). In addition to cropland expansion, land for dedicated bioenergy plantations is also located mostly in tropical forests and temperate forests and savannas. On the other hand, abandonment of pasture areas takes place mostly in tropical and temperate savannas and grasslands and tropical forests, leaving only temperate forests with a net increase of total agricultural area. At the global scale, landscapes with major LUC effects cover 13%–16% of the land surface by 2070–2099, slightly more than in the *INDC+* scenario (Figure 1). Major full impacts are projected for 54% (47%–61%) of the global land surface. During the second half of the 21st century, relatively low LUC impacts (compared to today and the other scenarios) can no longer compensate for increasing CC impacts, and *INDC* is likely to expose more landscapes to major impacts than either *Paris success* or *INDC+* in all biomes by 2070–2099 (Figure 3).

3.4. Paris Failure

More than half the land surface—54% with a model range of 48%–65%— is projected to experience major CC effects by 2070–2099 in the *Paris failure* scenario (Figure 1). This is roughly the same area as is projected to experience major impacts from both CC and LUC under the *INDC* scenario. Even though boreal forests may replace up to 97% of all tundra regions (Figure 3, ensemble mean 71%), increased mortality of boreal trees along their warm edge due to heat and water stress can often not be compensated fast enough by temperate tree recruitment, causing a wide-spread shift to a savanna-like state in both Russian and Canadian boreal regions (Figure S3 in the Supporting Information S1). The extent of biome transitions between tundra, boreal forests, and temperate savannas represents the largest area of climate-model related uncertainty in our simulations. Our findings are in general agreement with earlier studies that reported high risk of biome shifts in the high latitudes (e.g., Beck & Goetz, 2011; Gonzalez et al., 2010; Scholze et al., 2006), but responses were also found to differ considerably between vegetation models (e.g., Sitch et al., 2008; Warszawski et al., 2013). Major CC effects are also projected under the majority of climate models in large parts of the Amazon and African equatorial rainforests and South-east Asia (Figure 2). The underlying RCP8.5 features the largest total managed land of all four scenarios, with an increase of nearly 25% over present day (Table 1). At the global scale, landscape changes from LUC are still slightly lower than in the *Paris success* scenario, causing major impacts on 22% (21%–23%) of the land surface (Figure 1). They are particularly strong in South America, tropical Africa, India, and China, while LUC impacts decrease below present-day levels in parts of Europe and North America. Human interference with the biosphere through both CC and LUC is projected to put 73% (67%–80%) of the global land surface at risk of major landscape change by 2070–2099. Moderate changes ($0.1 < \Gamma < 0.3$) are simulated for another roughly 20% of the land surface, leaving a mere 3%–8% of ice-free landscapes worldwide with only minor biosphere changes.

While the Γ metric allows for a quantitative comparison of the magnitude of change its integrated value gives little indication of the type of change. Text S5 and Figure S7 in the Supporting Information S1 provide a decomposition of Γ into its components and illustrate the contributing factors to landscape change in different biomes. All results presented here use the area affected by $\Gamma > 0.3$ to aggregate impacts of CC and LUC at the landscape level to the biome or global scale, which essentially ignores landscapes with moderate or only minor impacts. In the Supporting Information S1, we test using the area-weighted global mean Γ as an alternative global measure (Text S6, Figure S8 of Supporting Information S1). This does not affect the ranking of scenarios relative to each other, but it does reduce the spread between scenarios. It also reduces the relative increase of impacts between the present-day state and the end of the scenario period. We also test the sensitivity of our results to the threshold used for Γ and find that most results are robust, except that lower thresholds reverse the ranking of *Paris success* and *INDC+* in terms of the full impact (Figure S9 of Supporting Information S1).

4. Discussion

We find that, with the exception of a full *Paris success*, CC is projected to take over as the main driver of major landscape change at the global scale by mid-century, and by the end of the century, major CC effects are projected for more than twice the area that experiences major LUC effects (Figure 1). In the *Paris success* case, CC roughly catches up with LUC. This finding is in qualitative agreement with earlier studies that found stronger effects of CC than LUC on biome distribution during the 21st century (Boit et al., 2016; Davies-Barnard et al., 2015). Two of the scenarios studied here, *Paris success* and *INDC+*, expose almost the same amount of areas worldwide to major change despite roughly 0.8 K difference in global mean temperature rise. CC impacts that are avoided under *Paris success* are compensated by LUC impacts which are higher than in all the other three studied scenarios. While this finding might suggest that strong climate mitigation (*Paris success*) provides no benefits—and may even cause more harm—to the terrestrial biosphere compared to the less ambitious *INDC+* scenario it is important to have a closer look at the underlying scenarios to understand whether the differences are indeed a result of the level of climate mitigation ambition or caused by other factors. In the RCP development process, each RCP scenario was constructed by a different IAM modeling group (van Vuuren et al., 2011a). While RCP8.5 represents a high-emission "baseline" scenario without any CC policies (Riahi et al., 2011), all the other IAMs used their own unique baseline conditions and then added climate mitigation measures to limit global warming in the most cost-efficient way (Masui et al., 2011;Thomson et al., 2011 ; van Vuuren et al., 2011b). As such, the baseline scenarios differ regarding key socioeconomic driving forces such as population, economic and income development, energy and land use (van Vuuren et al., 2011a). For example, the reference scenario for RCP4.5 (*INDC+*) has approximately 20% more agricultural land than the reference scenario for RCP2.6 (*Paris success*) (Thomson et al., 2011; van Vuuren et al., 2011b). RCP4.5 uses a universal carbon tax to induce reductions in GHG emissions from baseline conditions which applies equally to all emissions regardless of the source (industry, energy, land use) and creates a strong financial incentive in the IAM to avoid land use expansion and even leads to a large increase in forest extent (Wise et al., 2009a, 2009b), while still fulfilling food demand by shifting cropland to higher-yielding regions and shifting toward food products with a smaller carbon footprint (Thomson et al., 2010, 2011). As such, the reductions in global cropland and pasture areas (see Table 1) are an integral part of the mitigation strategy of the *INDC+* scenario, working in addition to the use of bioenergy to reduce emissions. It appears that no similar mechanism is present in RCP2.6 (*Paris success*) because mitigation from baseline conditions leads to an overall increase of the agricultural area, caused by an expansion of bioenergy (and BECCS), which is higher than in *INDC+*, and cropland expansion to balance a climate-driven reduction of crop productivity assumed in the IAM (van Vuuren et al., 2011b). An assessment of the technological assumptions made in the IAMs or the general feasibility of mitigation strategies in the RCPs is far beyond the scope of this analysis, but the lower agricultural area in RCP4.5 does not appear to be caused by different baseline assumptions in RCP2.6 and RCP4.5, but rather by the question how land use policies are affected by climate policy in each IAM.

Since the development of the original RCP scenarios, the CC research and the land system science community have collaborated to produce a new set of harmonized socioeconomic scenarios, the so-called Shared Socioeconomic Pathways (SSPs). The SSPs comprise five baseline scenarios describing alternative narratives for the 21st century, including sustainable development, regional rivalry, inequality, fossil-fueled development, and middle-of-the-road development, and IAM groups were asked to develop mitigation scenarios consistent with each baseline leading to each of the radiative forcing levels of the RCPs (Riahi et al., 2017). The SSP LUC scenarios should allow for a more systematic assessment of LUC impacts in the different RCPs (Popp et al., 2017); however, they are currently available from the SSP database (https://secure.iiasa.ac.at/web-apps/ene/SspDb/) only at the spatial disaggregation level of five world regions which makes them unsuitable for an impact assessment such as ours.

To allow for a more robust assessment of the impacts of future LUC, scenarios would need to provide more detailed information. For example, no information on crop irrigation is included in the RCP scenarios. Irrigated crops currently account for 33% of total crop production even though only 16% of global cropland is actually irrigated (Siebert et al., 2010; Siebert & Döll, 2010), and irrigation represents the largest human freshwater use accounting for approximately 70% of all human water withdrawals and approximately 90% of freshwater consumption (e.g., Döll et al., 2012; FAO, 2012). We use present-day irrigated areas and scale them linearly with future changes in total cropland to derive future irrigated areas (see subsection 2.1 of the

Methods). Given the required increase in crop productivity, we likely underestimate irrigation requirements especially in the *INDC+* scenario. Although water abstractions already exceed local renewable supplies in some regions, which may hamper future irrigation expansion (e.g., Döll et al., 2014; Vörösmarty et al., 2005), Jägermeyr et al. (2016) estimate a huge potential to increase crop production through integrated crop water management: combining irrigation efficiency improvements and low-tech solutions for small-scale farmers on water-limited croplands they calculate possible increases of global production of more than 40% if these measures were applied globally, all without increasing water withdrawals or expanding total cropland. The RCP scenarios also lack information on fertilizer use. Intensification has been a major driver of crop production increases during the second half of the 20th century, facilitated among other factors by a 500% increase in fertilizer use (FAO, 2016; Foley et al., 2011; Tilman et al., 2001). Low fertilizer use in many developing countries, especially Sub-Saharan Africa, is a chief reason for large yield gaps existing in these regions, providing both opportunities for and challenges to future crop production increases (Bruinsma, 2003; Cassman et al., 2005; IAASTD, 2009). At the other end of the spectrum, leaching and atmospheric emissions of excess nitrogen cause acidification and eutrophication in aquatic ecosystems, and high nitrogen deposition may induce species composition changes, enhance susceptibility to stress, cause direct foliar damage, and as a whole is linked to reduced plant species richness in many terrestrial ecosystems (Bobbink et al., 2010; Dise et al., 2011; Erisman et al., 2013).

These observations illustrate that the LUC scenarios underlying analysis such as our present study are a source of considerable uncertainty: their dependence on assumptions about global developments regarding increases in population, per capita demand, agricultural technology and management, policy measures influencing land use patterns and their consistency with co-evolving climate policy, interregional trade-offs etc., coupled with considerable model-structural and data-driven uncertainty, is difficult to overcome in a spatially explicit manner for a comprehensive assessment (e.g., Prestele et al., 2016).

5. Conclusions

We show that, together, CC and LUC risk causing major ecosystem change in landscapes covering 38%–80% of the global land surface by the end of the 21st century. While LUC is currently the major anthropogenic pressure on the terrestrial biosphere at the global scale, we find that it will likely be outpaced by CC in the second half of this century unless global warming can be limited to well below 2°C. The large uncertainty range of impacts is caused primarily by the span of climate outcomes analyzed here: major CC impacts are projected for 16%–27% of the land surface in the most ambitious *Paris success* scenario, but for 48%–65% of the land surface in case of a *Paris failure*. In comparison, the best and worst-case scenario in terms of LUC impacts, *INDC+* and *Paris success*, are projected to cause major impacts on 11%–13% and 22%–25% of the land surface, respectively.

Our analysis is restricted by the limited availability of land use scenarios of sufficient spatial and topical detail. Since the RCPs, research has gone into assessing and ultimately reducing the sources of uncertainties in future LUC projections (e.g., Prestele et al., 2016; Schmitz et al., 2014; Verburg et al., 2013), but also into a better representation of sustainability aspects (e.g., Godfray & Garnett, 2014; Verburg et al., 2015). The new SSP scenarios address some of the limitations of the original RCP scenarios discussed above. A subset of these scenarios will be disaggregated to a harmonized gridded resolution as a contribution of the Land Use Model Intercomparison Project (LUMIP) to CMIP6 (Lawrence et al., 2016). Similar to the RCP LUC scenarios within CMIP5, evaluation of the SSP scenarios with coupled climate-carbon cycle models will then allow for the quantification of biogeophysical impacts of LUC such as albedo changes through afforestation which, in contrast to biogeochemical impacts, are not accounted for by IAMs. For the time being, the RCP scenarios represent the best available set of internally consistent scenarios of future CC and LUC.

Despite large uncertainties, our results emphasize the importance of ambitious climate mitigation in the pursuit of limiting humanity's impact on the terrestrial biosphere. While IAM simulations suggest that low warming scenarios can be achieved following a range of socioeconomic and technology assumptions we show that these very development pathways play an important role in determining future land use and therefore the full impact of humanity on ecosystems. According to our simulations, the focus on preservation and restoration of nonagricultural ecosystems (mostly forests) in the *INDC+* scenario may be able to "offset" substantial additional warming compared to the more land-intensive *Paris success* scenario,

assuming that the large productivity increases required under *INDC+* can be achieved sustainably. To ensure that the Paris Agreement is a full success for the biosphere a co-transformation of the energy system (toward "clean" sources and efficiency improvements that limit CC) and the land use system (toward sustainable intensification that avoids and even reverses land expansion) will be required. Strategies proposed to achieve the latter include closing yield gaps in under-performing regions, increasing agricultural resource efficiency, diet shifts, and reducing waste (Foley et al., 2011). However, even if a *Paris success* for climate could be combined with an optimistic *INDC+*-like land use scenario this would not be able to fully prevent a substantial expansion of areas with major human interference with the biosphere compared to today.

Acknowledgments
S.O. was supported by the German Federal Ministry for the Environment, Nature Conservation and Nuclear Safety (16_II_148_Global_A_IMPACT). L.R.B. was supported by the German Research Foundation's priority program DFG SPP 1689 on "Climate Engineering – Risks, Challenges and Opportunities?" and specifically the CE-LAND project. S.S. was supported by the German Federal Ministry of Education and Research's (BMBF's) project "PalMod 2.3 Methankreislauf, Teilprojekt 2 Modellierung der Methanemissionen von Feucht- und Permafrostgebieten mit Hilfe von LPJmL" (Code 01LP1507C). The publication of this article was partially funded by the Open Access Fund of the Leibniz Association. We acknowledge the World Climate Research Programme's Working Group on Coupled Modeling, which is responsible for CMIP, and we thank the climate modeling groups for producing and making available their model output. For CMIP the U.S. Department of Energy's Program for Climate Model Diagnosis and Intercomparison provides coordinating support and led development of software infrastructure in partnership with the Global Organization for Earth System Science Portals. Bias correction of climate model output was kindly provided by Jens Heinke. Other data used are listed in the references, tables, and supporting information. Data underlying the analyses will be provided upon request to ostberg@pik-potsdam.de. The authors declare that they have no competing interests.

References

Beck, P. S. A., & Goetz, S. J. (2011). Satellite observations of high northern latitude vegetation productivity changes between 1982 and 2008: Ecological variability and regional differences. *Environmental Research Letters*, *6*(4), 045501. https://doi.org/10.1088/1748-9326/6/4/045501

Becker, A., Finger, P., Meyer-Christoffer, A., Rudolf, B., Schamm, K., Schneider, U., & Ziese, M. (2013). A description of the global land-surface precipitation data products of the Global Precipitation Climatology Centre with sample applications including centennial (trend) analysis from 1901–present. *Earth System Science Data*, *5*, 71–99. https://doi.org/10.5194/essd-5-71-2013

Beringer, T., Lucht, W., & Schaphoff, S. (2011). Bioenergy production potential of global biomass plantations under environmental and agricultural constraints. *GCB Bioenergy*, *3*, 299–312. https://doi.org/10.1111/j.1757-1707.2010.01088.x

Biemans, H., Haddeland, I., Kabat, P., Ludwig, F., Hutjes, R. W. A., Heinke, J., … Gerten, D. (2011). Impact of reservoirs on river discharge and irrigation water supply during the 20th century. *Water Resources Research*, *47*, W03509. https://doi.org/10.1029/2009WR008929

Bobbink, R., Hicks, K., Galloway, J., Spranger, T., Alkemade, R., Ashmore, M., … De Vries, W. (2010). Global assessment of nitrogen deposition effects on terrestrial plant diversity: A synthesis. *Ecological Applications*, *20*, 30–59. https://doi.org/10.1890/08-1140.1

Boit, A., Sakschewski, B., Boysen, L., Cano-Crespo, A., Clement, J., Garcia-Alaniz, N., … Thonicke, K. (2016). Large-scale impact of climate change vs. land-use change on future biome shifts in Latin America. *Global Change Biology*, *22*, 3689–3701. https://doi.org/10.1111/gcb.13355

Bondeau, A., Smith, P. C., Zaehle, S., Schaphoff, S., Lucht, W., Cramer, W., … Smith, B. (2007). Modelling the role of agriculture for the 20th century global terrestrial carbon balance. *Global Change Biology*, *13*, 679–706. https://doi.org/10.1111/j.1365-2486.2006.01305.x

Bruinsma, J. (Ed.) (2003). *World Agriculture : Towards 2015 / 2030 – An FAO Perspective*, 444 pp. London, England: Earthscan Publications Ltd.

Cassman, K. G., Wood, S., Choo, P. S., Cooper, H. D., Devendra, C., Dixon, J., … Tharme, R. (2005). Chapter 26: Cultivated systems. In A. Balisacan & P. Gardiner (Eds.), *Ecosystems and human well-being: Current state & trends* (Vol. *1*, pp. 745–794). Washington, DC: Island Press.

Collins, M., Knutti, R., Arblaster, J., Dufresne, J.-L., Fichefet, T., Friedlingstein, P., … Wehner, M. (2013). Chapter 12: Long-term climate change: Projections, commitments and irreversibility. In T. Stocker, D. Qin, G.-K. Plattner, M. Tignor, S. Allen, J. Boschung, et al. (Eds.), *Climate change 2013: The Physical Science Basis. Contribution of Working Group I to the Fifth Assessment Report of the Intergovernmental Panel on Climate Change* (pp. 1029–1136). Cambridge, England: Cambridge University Press.

Davies-Barnard, T., Valdes, P. J., Singarayer, J. S., Wiltshire, A. J., & Jones, C. D. (2015). Quantifying the relative importance of land cover change from climate and land use in the representative concentration pathways. *Global Biogeochemical Cycles*, *29*, 842–853. https://doi.org/10.1002/2014GB004949

Dise, N. B., Ashmore, M., Belyazid, S., Bleeker, A., Bobbink, R., de Vries, W., … van den Berg, L. (2011). Chapter 20: Nitrogen as a threat to European terrestrial biodiversity. In M. A. Sutton, C. M. Howard, J. W. Erisman, G. Billen, A. Bleeker, P. Grennfelt, & H. van Grinsven (Eds.), *The European nitrogen assessment* (pp. 463–494). Cambridge, England: Cambridge University Press. https://doi.org/10.1017/CBO9780511976988.023

Dlugokencky, E., and Tans, P. (2017). Trends in atmospheric carbon dioxide. National Oceanic & Atmospheric Administration, Earth System Research Laboratory (NOAA/ESRL). Retrieved from: https://www.esrl.noaa.gov/gmd/ccgg/trends/global.html.

Döll, P., Hoffmann-Dobrev, H., Portmann, F. T., Siebert, S., Eicker, A., Rodell, M., … Scanlon, B. R. (2012). Impact of water withdrawals from groundwater and surface water on continental water storage variations. *Journal of Geodynamics*, *59-60*, 143–156. https://doi.org/10.1016/j.jog.2011.05.001

Döll, P., Müller Schmied, H., Schuh, C., Portmann, F. T., & Eicker, A. (2014). Global-scale assessment of groundwater depletion and related groundwater abstractions: Combining hydrological modeling with information from well observations and GRACE satellites. *Water Resources Research*, *50*, 5698–5720. https://doi.org/10.1002/2014WR015595

Ellis, E. C., Klein Goldewijk, K., Siebert, S., Lightman, D., & Ramankutty, N. (2010). Anthropogenic transformation of the biomes, 1700 to 2000. *Global Ecology and Biogeography*, *19*(5), 589–606. https://doi.org/10.1111/j.1466-8238.2010.00540.x.

Ellis, E. C., & Ramankutty, N. (2008). Putting people in the map: Anthropogenic biomes of the world. *Frontiers in Ecology and the Environment*, *6*(8), 439–447. https://doi.org/10.1890/070062

Erisman, J. W., Galloway, J. N., Seitzinger, S., Bleeker, A., Dise, N. B., Petrescu, A. M. R., … de Vries, W. (2013). Consequences of human modification of the global nitrogen cycle. *Philosophical Transactions of the Royal Society of London. Series B, Biological Sciences*, *368*, 20130116. https://doi.org/10.1098/rstb.2013.0116

Fader, M., Rost, S., Müller, C., Bondeau, A., & Gerten, D. (2010). Virtual water content of temperate cereals and maize: Present and potential future patterns. *Journal of Hydrology*, *384*, 218–231. https://doi.org/10.1016/j.jhydrol.2009.12.011

FAO. (2012). Coping with water scarcity – An action framework for agriculture and food security. 79 pp., Food and Agriculture Organization of the United Nations, Rome. Retrieved from: http://www.fao.org/docrep/016/i3015e/i3015e.pdf.

FAO. (2014). AQUASTAT database. Food and Agriculture Organization of the United Nations, Rome. Retrieved from: http://www.fao.org/nr/water/aquastat/data/query/index.html?lang=en.

FAO. (2016). FAOSTAT database. Food and Agriculture Organization of the United Nations, Rome. Retrieved from: http://www.fao.org/faostat/en/.

FAO, IIASA, ISRIC, ISSCAS, and JRC. (2012). Harmonized World Soil database (version 1.2), Retrieved from: http://webarchive.iiasa.ac.at/Research/LUC/External-World-soil-database/HTML/.

Fawcett, A. A., Iyer, G. C., Clarke, L. E., Edmonds, J. A., Hultman, N. E., McJeon, H. C., … Shi, W. (2015). Can Paris pledges avert severe climate change? *Science*, *350*, 1168–1169. https://doi.org/10.1126/science.aad5761

Foley, J. A., Ramankutty, N., Brauman, K. A., Cassidy, E. S., Gerber, J. S., Johnston, M., … Zaks, D. P. M. (2011). Solutions for a cultivated planet. *Nature*, *478*, 337–342. https://doi.org/10.1038/nature10452

Gerten, D., Schaphoff, S., Haberlandt, U., Lucht, W., & Sitch, S. (2004). Terrestrial vegetation and water balance—Hydrological evaluation of a dynamic global vegetation model. *Journal of Hydrology*, *286*, 249–270. https://doi.org/10.1016/j.jhydrol.2003.09.029

GISTEMP Team (2017), GISS surface temperature analysis (GISTEMP). NASA Goddard Institute for Space Studies. Retrieved from: https://data.giss.nasa.gov/gistemp/.

Godfray, H. C. J., & Garnett, T. (2014). Food security and sustainable intensification. *Philosophical Transactions of the Royal Society B: Biological Sciences*, *369*(1639), 20120273. https://doi.org/10.1098/rstb.2012.0273

Gonzalez, P., Neilson, R. P., Lenihan, J. M., & Drapek, R. J. (2010). Global patterns in the vulnerability of ecosystems to vegetation shifts due to climate change. *Global Ecology and Biogeography*, *19*, 755–768. https://doi.org/10.1111/j.1466-8238.2010.00558.x.

Hansen, J., Ruedy, R., Sato, M., & Lo, K. (2010). Global surface temperature change. *Reviews of Geophysics*, *48*, RG4004. https://doi.org/10.1029/2010RG000345

Harris, I., Jones, P., Osborn, T., & Lister, D. (2014). Updated high-resolution grids of monthly climatic observations – The CRU TS3.10 dataset. *International Journal of Climatology*, *34*, 623–642. https://doi.org/10.1002/joc.3711

Heck, V., Gerten, D., Lucht, W., & Boysen, L. R. (2016). Is extensive terrestrial carbon dioxide removal a 'green' form of geoengineering? A global modelling study. *Global and Planetary Change*, *137*, 123–130. https://doi.org/10.1016/j.gloplacha.2015.12.008

Heinke, J., Ostberg, S., Schaphoff, S., Frieler, K., Müller, C., Gerten, D., … Lucht, W. (2013). A new climate dataset for systematic assessments of climate change impacts as a function of global warming. *Geoscientific Model Development*, *6*, 1689–1703. https://doi.org/10.5194/gmd-6-1689-2013

Heyder, U., Schaphoff, S., Gerten, D., & Lucht, W. (2011). Risk of severe climate change impact on the terrestrial biosphere. *Environmental Research Letters*, *6*, 034036. https://doi.org/10.1088/1748-9326/6/3/034036

Hoekstra, A. (1998). *Perspectives on water: An integrated model-based exploration of the future* (1st edition, 356 pp. ed.). Utrecht, The Netherlands: International Books.

Hurtt, G. C., Chini, L. P., Frolking, S., Betts, R. A., Feddema, J., Fischer, G., … Wang, Y. P. (2011). Harmonization of land-use scenarios for the period 1500–2100: 600 years of global gridded annual land-use transitions, wood harvest, and resulting secondary lands. *Climatic Change*, *109*, 117–161. https://doi.org/10.1007/s10584-011-0153-2

IAASTD (2009). *Agriculture at a Crossroads: Global Report*, 606 pp. Washington, DC: Island Press.

IPCC (2014). Summary for policymakers. In O. Edenhofer, R. Pichs-Madruga, Y. Sokona, E. Farahani, S. Kadner, K. Seyboth, et al. (Eds.), *Climate change 2014: Mitigation of climate change. Contribution of Working Group III to the Fifth Assessment Report of the Intergovernmental Panel on Climate Change* (pp. 1–32). Cambridge, England: Cambridge University Press.

Jägermeyr, J., Gerten, D., Heinke, J., Schaphoff, S., Kummu, M., & Lucht, W. (2015). Water savings potentials of irrigation systems: Global simulation of processes and linkages. *Hydrology and Earth System Sciences*, *19*, 3073–3091. https://doi.org/10.5194/hess-19-3073-2015

Jägermeyr, J., Gerten, D., Schaphoff, S., Heinke, J., Lucht, W., & Rockström, J. (2016). Integrated crop water management might sustainably halve the global food gap. *Environmental Research Letters*, *11*, 025002. https://doi.org/10.1088/1748-9326/11/2/025002

Joos, F., & Spahni, R. (2008). Rates of change in natural and anthropogenic radiative forcing over the past 20,000 years. *Proceedings of the National Academy of Sciences*, *105*, 1425–1430. https://doi.org/10.1073/pnas.0707386105

Klein Goldewijk, K., & van Drecht, G. (2006). HYDE 3. Current and historical population and land cover. In A. F. Bouwman, T. Kram, & K. Klein Goldewijk (Eds.), *Integrated Modelling of Global Environmental Change. An Overview of IMAGE 2.4*. Bilthoven, The Netherlands: Netherlands Environmental Assessment Agency (MNP).

Lawrence, D. M., Hurtt, G. C., Arneth, A., Brovkin, V., Calvin, K. V., Jones, A. D., … Shevliakova, E. (2016). The Land Use Model Intercomparison Project (LUMIP) contribution to CMIP6: Rationale and experimental design. *Geoscientific Model Development*, *9*, 2973–2998. https://doi.org/10.5194/gmd-9-2973-2016

Le Quéré, C., Andrew, R. M., Canadell, J. G., Sitch, S., Korsbakken, J. I., Peters, G. P., … Zaehle, S. (2016). Global carbon budget 2016. *Earth System Science Data*, *8*, 605–649. https://doi.org/10.5194/essd-8-605-2016

Lehner, B., & Döll, P. (2004). Development and validation of a global database of lakes, reservoirs and wetlands. *Journal of Hydrology*, *296*, 1–22. https://doi.org/10.1016/j.jhydrol.2004.03.028

Lehner, B., Liermann, C. R., Revenga, C., Vörösmarty, C., Fekete, B., Crouzet, P., … Wisser, D. (2011). High-resolution mapping of the world's reservoirs and dams for sustainable river-flow management. *Frontiers in Ecology and the Environment*, *9*, 494–502. https://doi.org/10.1890/100125

Masui, T., Matsumoto, K., Hijioka, Y., Kinoshita, T., Nozawa, T., Ishiwatari, S., … Kainuma, M. (2011). An emission pathway for stabilization at 6 Wm^{-2} radiative forcing. *Climatic Change*, *109*, 59–76. https://doi.org/10.1007/s10584-011-0150-5

Millennium Ecosystem Assessment (2005). *Ecosystems and human well-being: Synthesis*. Washington, DC: Island Press.

Ostberg, S., Lucht, W., Schaphoff, S., & Gerten, D. (2013). Critical impacts of global warming on land ecosystems. *Earth System Dynamics*, *4*, 347–357. https://doi.org/10.5194/esd-4-347-2013

Ostberg, S., Schaphoff, S., Lucht, W., & Gerten, D. (2015). Three centuries of dual pressure from land use and climate change on the biosphere. *Environmental Research Letters*, *10*, 044011. https://doi.org/10.1088/1748-9326/10/4/044011

Popp, A., Calvin, K., Fujimori, S., Havlik, P., Humpenöder, F., Stehfest, E., … van Vuuren, D. P. (2017). Land-use futures in the shared socio-economic pathways. *Global Environmental Change*, *42*, 331–345. https://doi.org/10.1016/j.gloenvcha.2016.10.002

Portmann, F. T., Siebert, S., & Döll, P. (2010). MIRCA2000–global monthly irrigated and rainfed crop areas around the year 2000: A new high-resolution data set for agricultural and hydrological modeling. *Global Biogeochemical Cycles*, *24*, GB1011. https://doi.org/10.1029/2008GB003435

Prestele, R., Alexander, P., Rounsevell, M. D. A., Arneth, A., Calvin, K., Doelman, J., … Verburg, P. H. (2016). Hotspots of uncertainty in land-use and land-cover change projections: A global-scale model comparison. *Global Change Biology*, *22*(12), 3967–3983. https://doi.org/10.1111/gcb.13337

Riahi, K., Rao, S., Krey, V., Cho, C., Chirkov, V., Fischer, G., … Rafaj, P. (2011). RCP 8.5–A scenario of comparatively high greenhouse gas emissions. *Climatic Change*, *109*, 33–57. https://doi.org/10.1007/s10584-011-0149-y

Riahi, K., van Vuuren, D. P., Kriegler, E., Edmonds, J., O'Neill, B. C., Fujimori, S., … Tavoni, M. (2017). The shared socioeconomic pathways and their energy, land use, and greenhouse gas emissions implications: An overview. *Global Environmental Change*, *42*, 153–168. https://doi.org/10.1016/j.gloenvcha.2016.05.009

Rockström, J., Schellnhuber, H. J., Hoskins, B., Ramanathan, V., Schlosser, P., Brasseur, G. P., … Lucht, W. (2016). The world's biggest gamble. *Earth's Future*, *4*, 465–470. https://doi.org/10.1002/2016EF000392

Rogelj, J., den Elzen, M., Höhne, N., Fransen, T., Fekete, H., Winkler, H., … Meinshausen, M. (2016). Paris Agreement climate proposals need a boost to keep warming well below 2 °C. *Nature*, *534*, 631–639. https://doi.org/10.1038/nature18307.

Rost, S., Gerten, D., & Heyder, U. (2008). Human alterations of the terrestrial water cycle through land management. *Advances in Geosciences*, *18*, 43–50. https://doi.org/10.5194/adgeo-18-43-2008

Schaphoff, S., Heyder, U., Ostberg, S., Gerten, D., Heinke, J., & Lucht, W. (2013). Contribution of permafrost soils to the global carbon budget. *Environmental Research Letters*, *8*, 014026. https://doi.org/10.1088/1748-9326/8/1/014026

Schmitz, C., van Meijl, H., Kyle, P., Nelson, G. C., Fujimori, S., Gurgel, A., … Valin, H. (2014). Land-use change trajectories up to 2050: Insights from a global agro-economic model comparison. *Agricultural Economics*, *45*(1), 69–84. https://doi.org/10.1111/agec.12090

Schneider, U., Becker, A., Finger, P., Meyer-Christoffer, A., Rudolf, B., and Ziese, M. (2011). GPCC full data reanalysis version 6.0 at 0.5°: Monthly land-surface precipitation from rain-gauges built on GTS-based and historic data. https://doi.org/10.5676/DWD_GPCC/FD_M_V6_050.

Scholze, M., Knorr, W., Arnell, N. W., & Prentice, I. C. (2006). A climate-change risk analysis for world ecosystems. *Proceedings of the National Academy of Sciences of the United States of America*, *103*, 13116–13120. https://doi.org/10.1073/pnas.0601816103

Siebert, S., Burke, J., Faures, J. M., Frenken, K., Hoogeveen, J., Döll, P., & Portmann, F. T. (2010). Groundwater use for irrigation – A global inventory. *Hydrology and Earth System Sciences*, *14*, 1863–1880. https://doi.org/10.5194/hess-14-1863-2010.

Siebert, S., & Döll, P. (2010). Quantifying blue and green virtual water contents in global crop production as well as potential production losses without irrigation. *Journal of Hydrology*, *384*, 198–217. https://doi.org/10.1016/j.jhydrol.2009.07.031

Sitch, S., Huntingford, C., Gedney, N., Levy, P. E., Lomas, M. R., Piao, S. L., … Woodward, F. I. (2008). Evaluation of the terrestrial carbon cycle, future plant geography and climate-carbon cycle feedbacks using five dynamic global vegetation models (DGVMs). *Global Change Biology*, *14*, 2015–2039. https://doi.org/10.1111/j.1365-2486.2008.01626.x

Sitch, S., Smith, B., Prentice, I. C., Arneth, A., Bondeau, A., Cramer, W., … Venevsky, S. (2003). Evaluation of ecosystem dynamics, plant geography and terrestrial carbon cycling in the LPJ dynamic global vegetation model. *Global Change Biology*, *9*, 161–185. https://doi.org/10.1046/j.1365-2486.2003.00569.x

Steffen, W., Crutzen, P. J., & McNeill, J. R. (2007). The Anthropocene: Are humans now overwhelming the great forces of nature. *Ambio: A Journal of the Human Environment*, *36*, 614–621. https://doi.org/10.1579/0044-7447(2007)36[614:TAAHNO]2.0.CO;2

Sykes, M. T., Prentice, I. C., & Laarif, F. (1999). Quantifying the impact of global climate change on potential natural vegetation. *Climatic Change*, *41*, 37–52. https://doi.org/10.1023/A:1005435831549.

Taylor, K. E., Stouffer, R. J., & Meehl, G. A. (2012). An overview of CMIP5 and the experiment design. *Bulletin of the American Meteorological Society*, *93*, 485–498. https://doi.org/10.1175/BAMS-D-11-00094.1

Thomson, A. M., Calvin, K. V., Chini, L. P., Hurtt, G., Edmonds, J. A., Bond-Lamberty, B., … Janetos, A. C. (2010). Climate mitigation and the future of tropical landscapes. *Proceedings of the National Academy of Sciences*, *107*, 19,633–19,638. https://doi.org/10.1073/pnas.0910467107

Thomson, A. M., Calvin, K. V., Smith, S. J., Kyle, G. P., Volke, A., Patel, P., … Edmonds, J. A. (2011). RCP4.5: A pathway for stabilization of radiative forcing by 2100. *Climatic Change*, *109*, 77–94. https://doi.org/10.1007/s10584-011-0151-4

Thonicke, K., Venevsky, S., Sitch, S., & Cramer, W. (2001). The role of fire disturbance for global vegetation dynamics: Coupling fire into a dynamic global vegetation model. *Global Ecology and Biogeography*, *10*, 661–677. https://doi.org/10.1046/j.1466-822X.2001.00175.x.

Tilman, D., Fargione, J., Wolff, B., D'Antonio, C., Dobson, A., Howarth, R., … Swackhamer, D. (2001). Forecasting agriculturally driven global environmental change. *Science*, *292*, 281–284. https://doi.org/10.1126/science.1057544

UNFCCC. (2015). Synthesis report on the aggregate effect of the intended nationally determined contributions. FCCC/CP/2015/7, Bonn, Germany: UNFCCC Secretariat, 66 pp. Retrieved from: http://unfccc.int/resource/docs/2015/cop21/eng/07.pdf.

UNFCCC. (2016). Adoption of the Paris Agreement. FCCC/CP/2015/10/Add.1, Bonn, Germany: UNFCCC Secretariat, 36 pp. Retrieved from: http://unfccc.int/resource/docs/2015/cop21/eng/10a01.pdf.

United Nations, Department of Economic and Social Affairs, Population Division (UNPD) (2015). *World population prospects: The 2015 Revision*. New York, NY: United Nations.

University of East Anglia Climatic Research Unit, Jones, P. D., and Harris, I. C. (2013). CRU TS3.21: Climatic Research Unit (CRU) Time-Series (TS) Version 3.21 of High Resolution Gridded Data of Month-by-month Variation in Climate (Jan. 1901 – Dec. 2012). NCAS British Atmospheric Data Centre. https://doi.org/10.5285/D0E1585D-3417-485F-87AE-4FCECF10A992.

van Vuuren, D. P., Edmonds, J., Kainuma, M., Riahi, K., Thomson, A., Hibbard, K., … Rose, S. K. (2011a). The representative concentration pathways: An overview. *Climatic Change*, *109*, 5–31. https://doi.org/10.1007/s10584-011-0148-z

van Vuuren, D. P., Stehfest, E., den Elzen, M. G. J., Kram, T., van Vliet, J., Deetman, S., … van Ruijven, B. (2011b). RCP2.6: Exploring the possibility to keep global mean temperature increase below 2°C. *Climatic Change*, *109*, 95–116. https://doi.org/10.1007/s10584-011-0152-3

Verburg, P. H., Crossman, N., Ellis, E. C., Heinimann, A., Hostert, P., Mertz, O., … Zhen, L. (2015). Land system science and sustainable development of the earth system: A global land project perspective. *Anthropocene*, *12*, 29–41. https://doi.org/10.1016/j.ancene.2015.09.004

Verburg, P. H., Tabeau, A., & Hatna, E. (2013). Assessing spatial uncertainties of land allocation using a scenario approach and sensitivity analysis: A study for land use in Europe. *Journal of Environmental Management*, *127*, S132–S144. https://doi.org/10.1016/j.jenvman.2012.08.038

Vörösmarty, C. J., Fekete, B. M., Meybeck, M., & Lammers, R. B. (2000). Global system of rivers: Its role in organizing continental land mass and defining land-to-ocean linkages. *Global Biogeochemical Cycles*, *14*, 599–621. https://doi.org/10.1029/1999GB900092

Vörösmarty, C. J., Lévêque, C., Revenga, C., Bos, R., Caudill, C., Chilton, J., … Reidy, C. A. (2005). Chapter 7: Fresh water. In F. Rijsberman, R. Costanza, & P. Jacobi (Eds.), *Ecosystems and human well-being: Current state & trends* (Vol. *1*, pp. 165–207). Washington, DC: Island Press.

Waha, K., van Bussel, L. G. J., Müller, C., & Bondeau, A. (2012). Climate-driven simulation of global crop sowing dates. *Global Ecology and Biogeography*, *21*, 247–259. https://doi.org/10.1111/j.1466-8238.2011.00678.x

Warszawski, L., Friend, A., Ostberg, S., Frieler, K., Lucht, W., Schaphoff, S., … Schellnhuber, H. J. (2013). A multi-model analysis of risk of ecosystem shifts under climate change. *Environmental Research Letters*, *8*, 044018. https://doi.org/10.1088/1748-9326/8/4/044018

Watanabe, S., Kanae, S., Seto, S., Yeh, P. J.-F., Hirabayashi, Y., & Oki, T. (2012). Intercomparison of bias-correction methods for monthly temperature and precipitation simulated by multiple climate models. *Journal of Geophysical Research: Atmospheres*, *117*, D23114. https://doi.org/10.1029/2012JD018192

Wise, M., Calvin, K., Thomson, A., Clarke, L., Bond-Lamberty, B., Sands, R., … Edmonds, J. (2009a). Implications of limiting CO2 concentrations for land use and energy. *Science*, *324*, 1183–1186. https://doi.org/10.1126/science.1168475

Wise, M. A., Calvin, K. V., Thomson, A. M., Clarke, L. E., Bond-Lamberty, B., Sands, R. D., … Edmonds, J. A. (2009b). The implications of limiting CO2 concentrations for agriculture, land use, land-use change emissions and bioenergy, Tech. Rep. PNNL-17943, Richmond, VA: Pacific Northwest National Laboratory.